XV Portuguese Conference on Fracture, PCF 2016, 10-12 February 2016, Paço de Arcos, Portugal

Thermo-mechanical modeling of a high pressure turbine blade of an airplane gas turbine engine

P. Brandão[a], V. Infante[b], A.M. Deus[c]*

[a]Department of Mechanical Engineering, Instituto Superior Técnico, Universidade de Lisboa, Av. Rovisco Pais, 1, 1049-001 Lisboa, Portugal
[b]IDMEC, Department of Mechanical Engineering, Instituto Superior Técnico, Universidade de Lisboa, Av. Rovisco Pais, 1, 1049-001 Lisboa, Portugal
[c]CeFEMA, Department of Mechanical Engineering, Instituto Superior Técnico, Universidade de Lisboa, Av. Rovisco Pais, 1, 1049-001 Lisboa, Portugal

Abstract

During their operation, modern aircraft engine components are subjected to increasingly demanding operating conditions, especially the high pressure turbine (HPT) blades. Such conditions cause these parts to undergo different types of time-dependent degradation, one of which is creep. A model using the finite element method (FEM) was developed, in order to be able to predict the creep behaviour of HPT blades. Flight data records (FDR) for a specific aircraft, provided by a commercial aviation company, were used to obtain thermal and mechanical data for three different flight cycles. In order to create the 3D model needed for the FEM analysis, a HPT blade scrap was scanned, and its chemical composition and material properties were obtained. The data that was gathered was fed into the FEM model and different simulations were run, first with a simplified 3D rectangular block shape, in order to better establish the model, and then with the real 3D mesh obtained from the blade scrap. The overall expected behaviour in terms of displacement was observed, in particular at the trailing edge of the blade. Therefore such a model can be useful in the goal of predicting turbine blade life, given a set of FDR data.

Keywords: High Pressure Turbine Blade; Creep; Finite Element Method; 3D Model; Simulation.

* Corresponding author. Tel.: +351 218419991.
    E-mail address: amd@tecnico.ulisboa.pt

1. Introduction

In the field of aviation, commercial demands make it necessary for modern gas turbine engines to function under extreme conditions, with a constant drive to push usage time beyond the manufacturer's conservative recommendations, while keeping safety requirements. In any of such instances, critical sections of the engine will eventually be detrimentally affected. That is the case of the high pressure turbine (HPT), where temperatures are the highest in the entire engine (Nadeau 2013).

As with most modern high-performance gas turbine engines, the turbine inlet temperatures in turboprop engines must be raised in order to increase the power output and thermodynamic efficiency (Boyce 2002a), creating a demanding high temperature environment where HPT blades operate. In order to maintain mechanical integrity of the nickel base superalloy blades, both coating and cooling have to be applied to the airfoil (Boyce 2002b, Han 2004).

With the goal of studying the life cycle of the HPT blades, a regional airline operation was featured. This company operates within the Azores islands and also provides flights between São Miguel (in Azores) and Madeira island, as well as between the latter and Gran Canaria island, all these routes being within the North Atlantic region. Its fleet is comprised of four Bombardier DHC8-400 airliners, also known as the Dash 8 Q400, for which the PW150A engine under study was especially designed.

In order to accomplish this work, the in-flight conditions that are recorded on the Flight Data Record (FDR) of this airline operation were analyzed. Using that information, Finite Element Method (FEM) simulations were made and the level of creep deformation that these blades suffer was determined. In order to do this, three different cycles, referred to (using standard airport codes) as SJZ-TER, PDL-HOR and PDL-FNC, with periods of approximately 20 minutes, 1 hour and 2 hours respectively, were studied. With the 1-cycle modeling defined, several successive cycles were then applied and a basic trend was assumed. The differences between each type of flight pattern were then determined and rough predictions on the creep behavior of the HPT blades were made for their expected life of 3000 flight hours.

Nomenclature

b	Reference Dimension
E22	Vertical Strain
EDS	Energy Dispersive Spectroscopy
FDR	Flight Data Record
FEM	Finite Element Method
HPT	High Pressure Turbine
ITT	Inter Turbine Temperature
K_1	Temperature Dependent Material Constant
l	Width of the blade's base
n	Creep Stress Exponent
N	Number of blades
NH	Rotation Speed
r	Radius of the disc
S22	Vertical Stress
SEM	Scanning Electron Microscopy
T	Material Temperature
TIT	Turbine Inlet Temperature
U2	Vertical Displacement
$\dot{\varepsilon}_s$	Steady-State Creep Rate
σ	Stress

2. Methodology

In order to study the thermo-mechanical behaviour of such critical components of an aircraft gas turbine engine as HPT blades, it was important to have as much knowledge as possible about the blade, e.g. on the material, the geometry, as well as on the operating conditions within the engine (Infante et al. 2009). With that, a finite element model could be developed. Therefore, several procedures were followed, as described in the following sub-sections.

2.1. Flight Data Record Processing

Several flights of the four different aircraft where studied and the variations in Inter Turbine Temperature (ITT) and HPT rotation speed (NH) for each of the selected flights were obtained from the Flight Data Records (FDR). Through this data, the different flight cycle duration and the routes flown by each of these aircraft were determined, and after treatment of such data, the plots for the Turbine Inlet Temperature (TIT) in ºC and NH in radians per second were averaged from the several plots extracted from the FDR.

The TIT plots were obtained through the definition of a temperature differential between the highest allowable ITT (920 ºC) (Goto et al. 2010) and the maximum usual operating temperature for blades with cooling systems applied (1027.85 ºC) (Błachnio et al. 2011), so that this differential was simply added to the original ITT plot values. A cooling stage bringing the whole blade to a temperature of 20 ºC was also included.

2.2. Part Reverse Engineering

- Part Geometric Modeling

Given that no 3D model of the blade was available, a 3D scan was made from a scrap of the HPT blade seen in Fig. 1. (a). A polygon mesh of the HPT blade's surface was created in the scanner's software and then it was used as a visual aid in a 3D modeling software where, along with raw physical dimensional measurements of the scrap, the final 3D model of the blade, seen in Fig. 1. (b), was created. From the width of the blade's base in Fig. 1. (c), $l =$ 16.9 mm, and knowing that there are N = 41 blades in the HPT, by using Equation 1, the radius of the HPT disk is:

$$r = \frac{N.l}{2\pi} = 111 \, mm \tag{1}$$

This was later used to calculate the centrifugal force applied to the HPT blades in each instant.
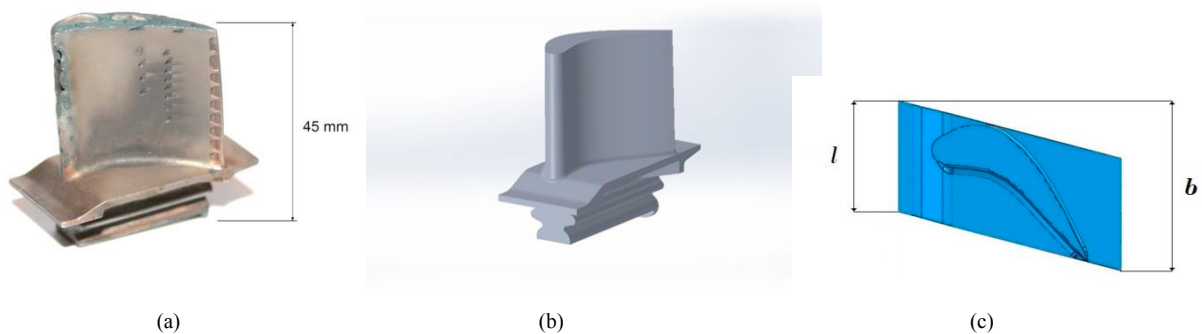

(a)　　　　　　　　　　　(b)　　　　　　　　　　　(c)

Fig. 1. (a) HPT blade scrap; (b) 3D model; (c) base width.

- Superalloy Composition

In order to determine the chemical composition of the scrap part, surface scanning electron microscopy (SEM) was performed as well as energy dispersive spectroscopy (EDS) analysis in the areas highlighted in Fig. 2. It can be

seen in Table 1 that the HPT blade is made of a nickel-based alloy with the expected ratio of chromium and cobalt typical of this type of superalloy. The varying concentration of both aluminum and platinum can easily be attributed to the base Pt-Al anti-corrosion coating usually found in these parts.
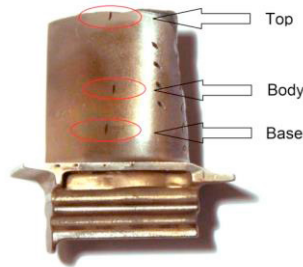

Fig. 2. HPT blade sections where SEM and EDS were performed.

Table 1. EDS analysis.

	Element Wt %						
	Al	Cr	Co	Ni	Ta	Fe	Pt
Top	3.36	1.99	8.68	74.87	2.27	-	8.84
Body	12.16	2.28	7.34	64.42	-	0.31	13.49
Base	2.53	0.59	7.06	64.91	-	-	24.91

- Superalloy Selection

From the composition found in the previous section, the type of superalloy that should be found in the available literature is determined, so the TMS-75 was considered (NIMS 2006), due to its Co/Cr ratio being approximately matched by the one measured in the previous section.

The creep rupture strength data was defined in terms of a steady-state creep rate, shown in Equation 2 (11) (Aghaie-Khafri et al. 2011), and the needed constants were obtained and defined in Table 2.

$$\dot{\varepsilon}_s = K_1 \sigma^n \tag{2}$$

Table 2. Steady state creep constants.

T (ºC)	K_1 (SI)	n (-)
900	5.575×10^{-23}	1.754
1100	9.062×10^{-22}	1.754
1150	1.610×10^{-21}	1.754

2.3. Finite Element Modeling

To properly study the behavior of the HPT blade in terms of creep deformation under centrifugal loading, the Abaqus™/Simulia™ FEM software suite was used, in order to simulate the different flight cycles discussed previously. This was done through the use of two different models: Rectangular Block Model and Blade Model.

- Rectangular Block Model

In order to test the methodology that would be later applied to the blade model, a simple rectangular block was created, using the basic dimensions of the airfoil geometry of the HPT blade (see Fig. 3. (a)). A thermal analysis was conducted on the model, and thermal boundary conditions as well as prescribed fields were created to simulate the thermal loading on the model's surface and the temperature variation between the surface and the interior of the part during the flight cycle. The surface temperatures in all the faces of the rectangular block, with the exception of its base, which was considered isolated from the hot gas flow, were made to vary according the TIT plot.

Using the nodal temperature distributions obtained from the heat transfer analysis as well as the variation in rotational speed during the flight cycle, a mechanical analysis was subsequently conducted, featuring the centrifugal forces experienced by the blade while in operation. Two different types of mechanical analysis were performed: in the first one, an elastoplastic analysis, a rotational body force was applied to the entire rectangular block with the rotation axis located 111 mm below the base, using an angular velocity derived from Equation 1, and centered along the 5 mm thickness of the rectangular block; then in the second, creep behavior was added.

Finally, in order to evaluate the influence of the variation of temperature along the interior of the rectangular block, two different isothermal analyses were conducted, one within the elastoplastic analysis and the other in the elastoplastic plus creep analysis. For this analysis, the TIT plotted data was used and applied to the entirety of the rectangular block and the part was considered isothermal.

- Blade Model

Once the methodology in the previous section was deemed appropriate, the same analyses were performed on the blade model (see Fig. 3. (b)), with just slight differences in some of its phases. To extract results, specific reference nodes were chosen (see Fig. 3. (c)). For the mechanical analysis the location of the rotation axis was centered along the midpoint of the largest dimension $b = 24.43$ mm (see Fig. 1. (c)). Different boundary conditions had to be defined separately, in order to simulate the way the actual HPT blade is seated on the HPT disk as well as the way in which the blades are set against each other.
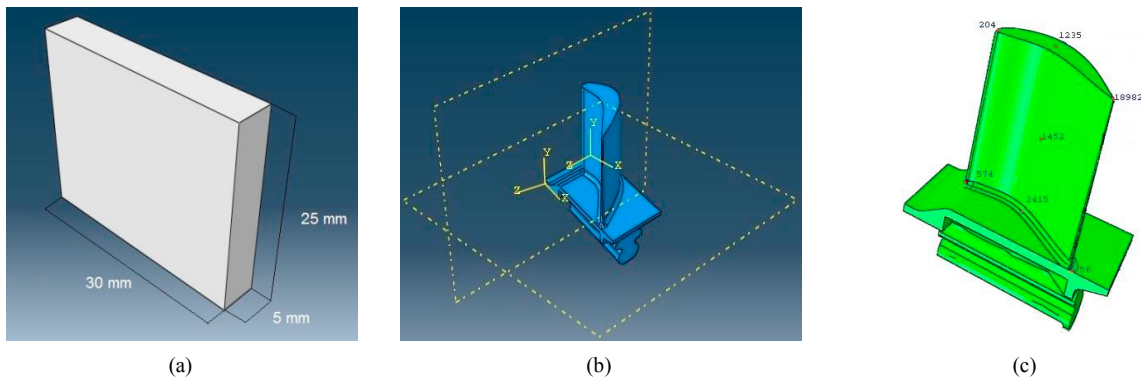

Fig. 3. (a) Rectangular Block Model; (b) Blade Model; (c) selected reference nodes.

3. Results and Discussion

3.1. Analyses Comparison

Studies were conducted in the Rectangular Block Model on the influence of considering the part isothermal, as opposed to considering the temperature time evolution and distribution between the part's surface and core, as well as the difference between the part's behaviour when comparing elastoplastic to creep conditions. Results are presented in Fig. 4., for only one cycle. Disregarding the temperature distribution showed small but noticeable changes in terms of vertical displacement (U2) of the part. Regarding creep versus elastoplastic behaviour, it will become obviously different at long times.
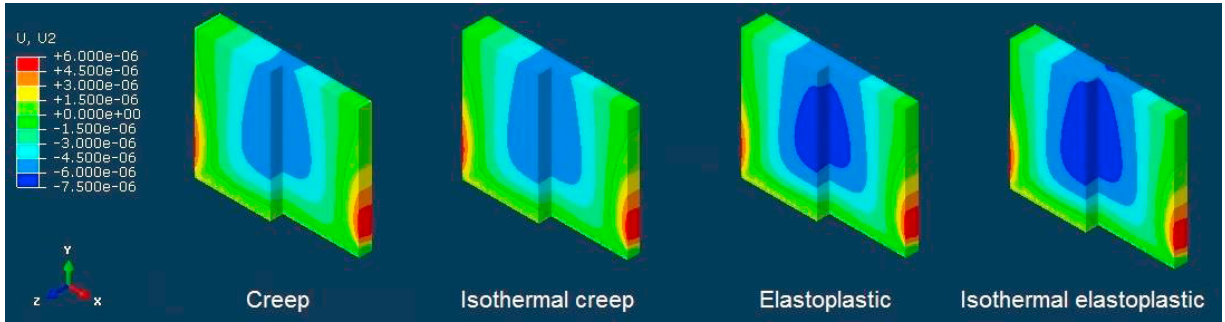
Fig. 4. Vertical displacement (U2) distribution for the four analyses performed.

3.2. Elastoplastic Analysis versus Creep Analysis

Comparisons between creep and elastoplastic analyses with the number of cycles increased were performed for both models, with 10 PDL-FNC flight cycles for the rectangular block model (see Fig. 5. (a)), and 5 DL-FNC flight cycles for the blade model (see Fig. 5. (b)). The differences in vertical displacement are noticeable, especially in the case of 10 cycles. Large displacements for elastoplastic cases are still to be expected, in view of the fact that the alloy is ductile.

In the case of the blade model, overall large differences in the distribution of vertical displacement were present, so the methodology for the creep analysis with the blade model was considered the best possible approximation to the behaviour of a real HPT blade.
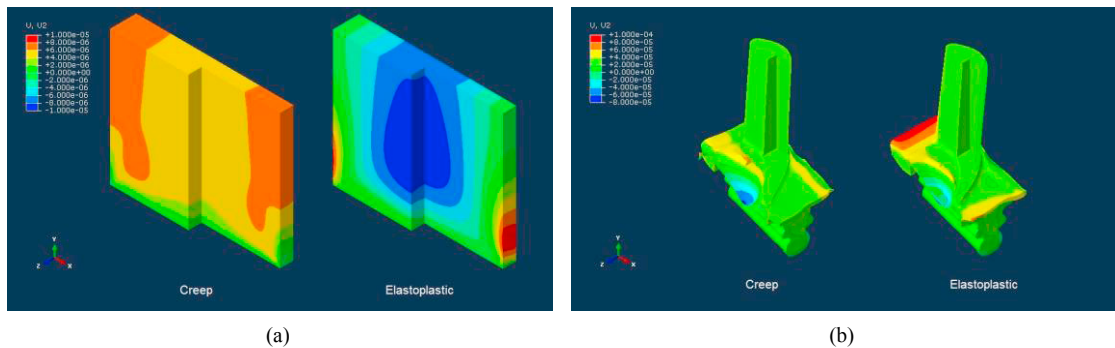

Fig. 5. Vertical displacement (U2) distribution after (a) 10 PDL-FNC flight cycles; (b) 5 PDL-FNC flight cycles.

3.3. Cycle Accumulation Analysis

In order to obtain an overall perception of the vertical displacement of the HPT blade during service, 10 successive cycles for the PDL-FNC flight cycle were ran. However, it was later realized that, by running 50 successive cycles, the first 10 were only descriptive of a transient phase for the overall trend of stretching of the parts. Therefore, if extrapolation procedures are taken, they must be carried out with caution.

The highest concentration of vertical stress is located in the bottom of the part, where it is connected to the HPT disk (see Fig. 6. (a)). The displacement of the trailing edge shown is in accordance with what is expected, although the retraction of the leading edge is somehow unexpected (Fig. 6. (b)) and merits future consideration. The vertical strain distribution is also shown (Fig. 6. (c)).

The same simulation performed for the PDL-FNC flight cycle was also carried out for both the PDL-HOR and SJZ-TER flight cycles (see Fig. 7). The first route presented larger amounts of displacement, followed in succession by the latter two, as expected, due to the decreasing cycle periods (8050, 4055 and 2050 seconds, respectively) and to the nature of creep as a function of time (Tin 2009, Epishin et al. 2010), with its effects being more noticeable for

the longer overall time spent at high temperatures during the 50 cycles.

In order to have a base approximation of the expected blade displacement after the 3000 hours period for each of the routes, the vertical displacement results for selected nodes were obtained from the fifty cycle analysis, as can be seen in Table 3. These values of vertical displacement are to be expected, given that, even though the PDL-FNC flight cycle is experienced less times, it remains at high temperature operating conditions for a longer period of the 3000 hours, when compared to the two other cycles, and thus it experiences the greater values in terms of overall displacement. This effect, however, seems to be less pronounced in areas where contraction, instead of expansion, occurs.

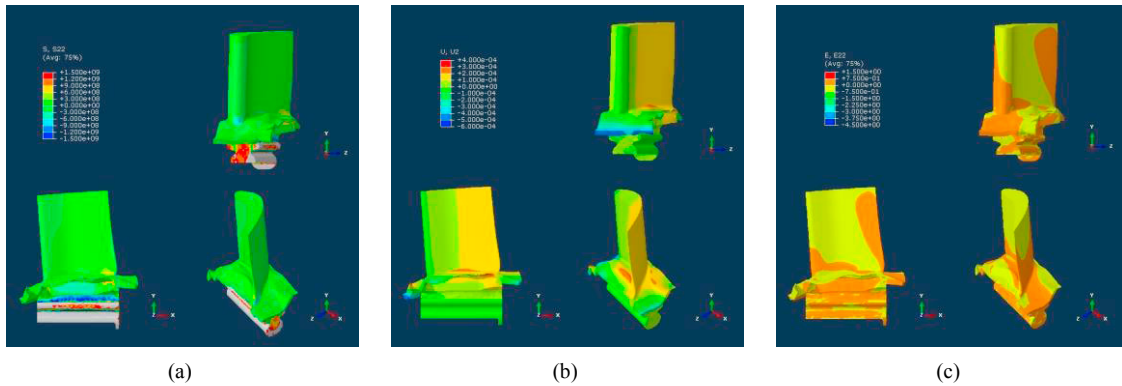| (a) | (b) | (c) |

Fig. 6. Distribution, after 50 PDL-FNC flight cycles, of (a) S22, vertical stress; (b) U2, vertical displacement; (c) E22, vertical strain.
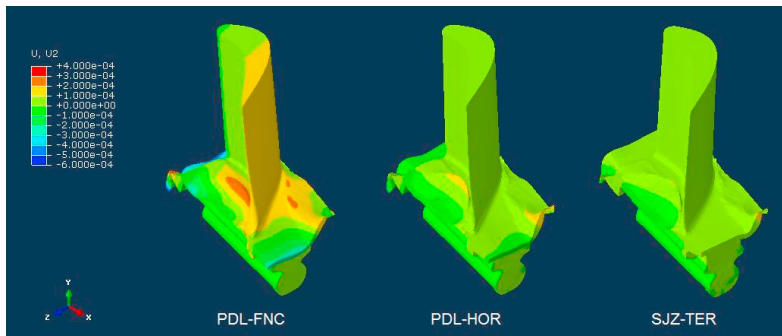

Fig. 7. Comparison between three different flight routes after 50 flight cycles (vertical displacement, U2).

Table 3. Nodal results for trend study of 3000 flight hours.

Flight Routes	Number of Cycles	Reference Node						
		18982	204	1235	1452	56	2415	574
		Displacement (m)						
PDL-FNC	1342	4.73E-3	-1.41E-3	1.99E-3	2.25E-3	9.14E-4	2.12E-3	-3.04E-3
PDL-HOR	2664	3.20E-3	-1.89E-3	4.88E-4	8.94E-4	1.18E-3	9.09E-4	-2.78E-3
SJZ-TER	5269	2.51E-3	-1.48E-3	-1.15E-4	4.27E-4	1.44E-3	4.65E-4	-1.96E-3

4. Summary and Conclusions

The main goal of this study was the development of a numerical model allowing for the analysis of the thermal and mechanical behaviour of a HPT blade, with emphasis on creep deformation.

A blade scrap part that was provided by a commercial airline was used, both in the definition of the dimensions necessary for the cycle simulation and the creation of a suitable 3D model of the blade. A suitable mesh for the FEM analysis was therefore obtained. As for the blade material, since the manufacturer declined to reveal its precise composition, a chemical analysis was carried out and a reasonable match was made with a specific nickel-based superalloy.

The choice of conducting trial simulations on a rectangular block model made it possible not only to compare isothermal with non-isothermal models, but also between elastoplastic and (elastoplastic plus) creep based models. It was seen that considering a temperature distribution along the part does affect results (as compared with an isothermal case). Therefore a thermal analysis should be performed before the mechanical analysis in order to obtain a more realistic simulation. Comparison between elastoplastic and elastoplastic + creep behaviors was also performed on the blade model.

The results for displacement in the blade models, after accumulation of the different flight cycles analyzed, show ever accumulating displacement on the trailing edge, which in time would lead to failure due to non-geometrical conformity; nevertheless, it was obtained a behavior that was not the expected in some parts of the blade, given that it was observed some instances of contraction, slight as it may be, especially in the leading edge. This seems to be an issue where further study is needed, especially in regards to the constitutive model of the blade material.

It was also verified that studies where creep behavior is extrapolated when a large number of flight cycles are involved should be undertaken with great care. The alternative is obviously to run simulations for whatever number of cycles needed.

The modeling approach seems to be adequate in providing a rough yet useful way to look at the creep behavior of a high pressure turbine blade of an airplane gas turbine engine.

Acknowledgements

References

Aghaie-Khafri, M., Noori, M., 2011. Life prediction of Ni-base superalloy. Bulletin of Materials Science 34(2), 305–309.

Błachnio, J., Pawlak, W.I., 2011. Damageability of Gas Turbine Blades – Evaluation of Exhaust Gas Temperature in Front of the Turbine Using a Non-Linear Observer, in "Advances in Gas Turbine Technology", Benini, E. (Ed.), InTech, 435-464.

Boyce, M.P., 2002a. An Overview of Gas Turbines, in "Gas Turbine Engineering Handbook", 2nd ed., Woburn, MA. Butterworth-Heinemann, 9–15.

Boyce, M.P., 2002b. Axial-Flow Turbines, in "Gas Turbine Engineering Handbook", 2nd ed., Woburn, MA. Butterworth-Heinemann, 351–363.

Epishin, A., Link, T., Klingelhöffer. H., Fedelich. B., Portella. P., 2010. Creep damage of single-crystal nickel base superalloys: Mechanisms and effect on low cycle fatigue. Materials at High Temperatures 27(1), 53–59.

Goto, N., Kusuki, Y., Endo, S., Toyooka, N., Shuto., Y., Matsuo, A., 2010. Aircraft Serious Incident Investigation Report. Japan Air Commuter Co., Ltd. Bombardier DHC-8-402, JA848C. Japan Transport Safety Board. Available: http://www.mlit.go.jp/jtsb/eng-air_report/JA848C.pdf (access on Jan 4, 2016).

Han, J., 2004. Recent Studies in Turbine Blade Cooling , International Journal of Rotating Machinery 10(6), 443-457.

Infante, V., Silva, J.M., de Freitas, M., Reis, L., 2009. Failures Analysis of Compressor Blades of Aeroengines due to Service, Engineering Failure Analysis 16(4), 1118-1125.

Nadeau, D.C., 2013. The Development of a Thermal Model to Predict Corrosion Propensity on Internal Features of Turbine Airfoils, Thesis, Rensselaer Polytechnic Institute, Hartford, CT.

NIMS report, 2006. Third Generation Nickel Base Single Crystal Superalloy Tms-75 (Tmd-103), High Temperature Materials Center, National Institute for Materials Science (NIMS). Available: http://sakimori.nims.go.jp/catalog/TMS75-TMD103-rev.pdf (access on Jan 4, 2016).

Tin, S., 2009. Modeling of Creep, in "ASM Handbook. Volume 22A Fundamentals of Modeling for Metals Processing", Furrer, D.U., Semiatin, S.L., Eds. ASM International, Materials Park, OH, p. 400–407.